

Z and Higgs boson decays with doubly-charged scalars at one-loop: current constraints, future sensitivities, and application to lepton-triality models.

Gabriela Lichtenstein^a, Michael A. Schmidt^a, German Valencia^b, Raymond R. Volkas^c

^a*Sydney Consortium for Particle Physics and Cosmology, School of Physics, The University of New South Wales, Sydney, New South Wales, 2052, Australia*

^b*School of Physics and Astronomy, Monash University, Wellington Road, Clayton, Victoria, 3800, Australia*

^c*ARC Centre of Excellence for Dark Matter Particle Physics, School of Physics, The University of Melbourne, Victoria, 3010, Australia*

Abstract

We analyse the Z and Higgs boson decays $Z \rightarrow \ell^+\ell^-$ ($\ell = e, \mu, \tau$), $H \rightarrow \gamma\gamma$ and $H \rightarrow Z\gamma$ that are induced at one-loop level in models with a doubly-charged isosinglet scalar. After discussing current constraints, we derive the parameter space that will be probed by the HL-LHC and the possible future colliders the ILC, CEPC and FCC. We then apply those constraints to lepton triality models which are based on a discrete Z_3 family symmetry and were recently studied in the context of charged-lepton flavour-violating processes at Belle II and the proposed $\mu^+\mu^+$ and μ^+e^- collider known as μ TRISTAN. We find that the future constraints that can be imposed by $Z \rightarrow \ell^+\ell^-$ on the lepton flavour conserving couplings of the triality models reduce the viable parameter space to probe lepton flavour violating processes. The constraints from Higgs boson decays are the first on the Higgs portal sector of the triality models.

1. Introduction

The phenomenology of doubly-charged scalars has been a topic of on-going interest [26, 18, 1, 35, 55, 54, 57, 42, 10, 11, 3, 67, 74]. In this paper, we study isosinglet doubly-charged scalars that couple to right-handed charged-lepton bilinears and induce contributions at one-loop level to the Higgs boson decays $H \rightarrow \gamma\gamma$, $Z\gamma$ and the Z boson decays $Z \rightarrow \ell^+\ell^-$ ($\ell = e, \mu, \tau$). As well as the general model of this kind, we also apply our results to specific realisations employing lepton triality (see below).

After computing the most up-to-date bounds from existing measurements of these processes, we also determine for the first time the parameter space reach of the High-Luminosity Large Hadron Collider (HL-LHC) [32], an International Linear Collider (ILC) [19, 20, 13], a Circular Electron Positron Collider (CEPC) [40, 43, 33], and a Future Circular Collider in both e^+e^- mode (FCC-ee) and through an integrated $ee/eh/hh$ program (FCC-int) [4, 24].

Email addresses: gabriela.lichtenstein@alumni.usp.br (Gabriela Lichtenstein), m.schmidt@unsw.edu.au (Michael A. Schmidt), german.valencia@monash.edu (German Valencia), raymondv@unimelb.edu.au (Raymond R. Volkas)

Our analysis goes beyond the recent analyses [26, 11] of a doubly-charged scalar which have been carried out as part of a more general study of single scalar particle extensions. Reference [26] did not include loop-level matching of the single scalar extensions onto SM effective field theory (SMEFT) and thus does not include all contributions to the leptonic Z -boson couplings. Reference [11] performed the matching onto SMEFT at the one-loop level and carried out a general study within SMEFT, but did not translate the general results in SMEFT back to the model parameters of the doubly-charged scalar. We further use the latest experimental results for Higgs decays and projections for future colliders in our analysis.

The general results are used to determine future experimental sensitivities and current constraints on specific isosinglet doubly-charged scalar models that utilise the discrete flavour symmetry of lepton triality.¹ These models are of interest because they serve as benchmarks for the phenomenological study of charged-lepton flavour-violating (CLFV) processes [25, 56]. They feature doubly-charged scalars with family-dependent Yukawa couplings to charged fermions that are dictated by lepton triality. The main motivation for studying these particular models is to provide simple exemplar theories where the dominant beyond Standard Model (BSM) effects are flavour-changing processes involving the τ lepton, in particular the decays $\tau^\pm \rightarrow \mu^\pm \mu^\pm e^\mp$ and $\tau^\pm \rightarrow e^\pm e^\pm \mu^\mp$ that will be probed with impressive sensitivity by Belle II [25]. Another phenomenological analysis [56] compared the Belle II reach from τ decays with complementary bounds from charged-lepton scattering processes that could eventually be obtained using the proposed $\mu^+ \mu^+$ and $\mu^+ e^-$ collider facility known as μ TRISTAN [47].

The remainder of this paper is structured as follows. Section 2 introduces the doubly-charged scalar extension of the SM, reviews the isosinglet triality models of Ref. [25] and summarises the currently known experimental bounds. Section 3 then derives constraints from the one-loop contributions to $Z \rightarrow \ell^+ \ell^-$, $H \rightarrow \gamma \gamma$ and $H \rightarrow Z \gamma$ based on existing data, and also determines the parameter-space reach of HL-LHC, ILC and FCC. Section 4 is a conclusion. Some technical details are provided in the Appendices.

2. Doubly-charged scalar models

2.1. General model

We consider a colourless doubly-charged isosinglet scalar k with Yukawa interactions

$$\mathcal{L}_k = \frac{1}{2} y_{ij} \overline{(e_{iR})^c} e_{jR} k + \text{h.c.} \quad (1)$$

The Yukawa coupling matrix y is symmetric in the flavour indices, $y_{ij} = y_{ji}$. We denote the mass of the exotic scalar by m_k . The scalar k also couples to the SM Higgs doublet ϕ via the quartic Higgs portal interaction, and of course also to the photon A^μ and the Z -boson Z^μ . The relevant non-Yukawa interaction terms are

$$\mathcal{L} \supset |D_\mu k|^2 - m_k^2 k^\dagger k - \frac{\lambda_k}{2} (k^\dagger k)^2 - \kappa_\phi \left(\phi^\dagger \phi - \frac{v^2}{2} \right) k^\dagger k - \frac{\lambda}{2} \left(\phi^\dagger \phi - \frac{v^2}{2} \right)^2 \quad (2)$$

¹Lepton triality may appear as an approximate symmetry in more complete lepton flavour discrete symmetry models; see e.g. Refs. [9, 49, 5, 6, 31, 50, 64, 61].

where $D_\mu = \partial_\mu + i2e(A_\mu - \tan\theta_W Z_\mu)$ is the covariant derivative, with θ_W being the weak mixing angle, e the electromagnetic coupling constant, λ the quartic SM Higgs interaction, λ_k the quartic k interaction, $v = (\sqrt{2}G_F)^{-1/2} \simeq 246$ GeV the SM Higgs vacuum expectation value, and κ_ϕ the Higgs portal coupling constant between the SM Higgs doublet and k . In unitary gauge after electroweak symmetry breaking $\phi^\dagger\phi = (v+H)^2/2$, where H denotes the Higgs field. Perturbative unitarity constrains the Yukawa couplings to be smaller than $\sqrt{4\pi}$ and the scalar couplings $|\lambda_k| \leq 4\pi$ and $|\kappa_\phi| \leq 8\pi$. The stability of the scalar potential requires $\lambda, \lambda_k > 0$ and $\kappa_\phi > -\sqrt{\lambda\lambda_k} > -\sqrt{4\pi}m_H/v \simeq -1.8$; see e.g. [52], where we used the perturbative unitarity bound for λ_k in the last inequality.²

The specific class of doubly-charged isosinglet scalar models utilising lepton triality is briefly reviewed next.

2.2. Brief review of the lepton triality models

The Z_3 flavour symmetry of lepton triality acts solely on leptons via the transformations

$$L \rightarrow \omega^T L, \quad e_R \rightarrow \omega^T e_R \quad (3)$$

where $T = 1, 2, 3$ for the first, second and third families, respectively, and $\omega = e^{2\pi i/3}$ is a cube root of unity. This means that e and ν_e transform multiplicatively via ω , μ and ν_μ transform via ω^2 , while τ and ν_τ are singlets. The charged-lepton Yukawa and mass matrices are forced to be diagonal. See Ref. [25] for a brief discussion of neutrino mass generation within the lepton triality models.

The models we consider all contain a single colourless, isosinglet, doubly-charged scalar. There are three models, each containing one of the positive doubly-charged scalars k_1, k_2 or k_3 , with

$$k_1 \rightarrow \omega k_1, \quad k_2 \rightarrow \omega^2 k_2 \quad \text{and} \quad k_3 \rightarrow k_3 \quad (4)$$

under triality. We refer to these as the $T = 1$, $T = 2$ and $T = 3$ models, respectively.³ We denote the masses of the exotic scalars by m_{k_1} , m_{k_2} and m_{k_3} .

Triality constrains the allowed Yukawa interactions from Eq. (1): k_1 is restricted to $y_{32} = y_{23} \equiv f_1$ and $y_{11} \equiv f_2$ with all others vanishing; k_2 has $y_{31} = y_{13} \equiv g_1$ and $y_{22} \equiv g_2$ with the rest being zero; and k_3 has $y_{21} = y_{12} \equiv h_1$ and $y_{33} \equiv h_2$ only. The coupling constants $f_{1,2}$, $g_{1,2}$ and $h_{1,2}$ may be taken to be real and non-negative without loss of generality.

2.3. Existing constraints

We now very briefly summarise some existing experimental constraints – see Refs. [25, 56] for further discussion, especially in the context of the lepton triality models.

There are two analyses using LHC data of direct searches for doubly-charged scalars decaying to same-sign charged lepton pairs, including flavour-violating modes. First, ATLAS [1]

²The study of vacuum stability dependence on the renormalisation scale depends on unknown ultraviolet physics which we expect to be present and thus it is beyond the scope of this work.

³The isotriplet models introduced in Ref. [25] will not be considered in this paper, but would be interesting to examine in future work.

conducted a search with an integrated luminosity of 36 fb^{-1} of data for the pair production of doubly-charged scalar singlets decaying to $\ell^\pm \ell^\pm$. Not seeing a signal, they derived direct lower bounds on the scalar masses. The precise bounds depend on assumptions about the branching ratios, but they are in the approximate range of $0.55 - 0.75 \text{ TeV}$ for typical benchmark choices. Second, as discussed previously in Ref. [56], the latest ATLAS searches [3] using an integrated luminosity of 139 fb^{-1} obtained an improved lower bound of 0.9 TeV on the doubly-charged scalar mass in the Zee-Babu model [75, 17] for the special case of universal lepton couplings. This limit applies to the doubly-charged scalars in triality models if they decay to same-sign leptons with equal probability for different flavours, which is not the general situation. In the absence of precise bounds expressed as functions of different branching ratios for the 139 fb^{-1} analysis, we show two *indicative* bounds in the later plots, labelled by the integrated luminosities 36 fb^{-1} and 139 fb^{-1} .

Reference [25] analysed existing Belle constraints on the CLFV decay modes of the τ , producing the bounds

$$\sqrt{f_1 f_2} \lesssim 0.17 \frac{m_{k_1}}{\text{TeV}} \quad \text{and} \quad \sqrt{g_1 g_2} \lesssim 0.17 \frac{m_{k_2}}{\text{TeV}}, \quad (5)$$

with the future sensitivity of Belle II [25] determined to be

$$\sqrt{f_1 f_2} \lesssim 0.06 \frac{m_{k_1}}{\text{TeV}} \quad \text{and} \quad \sqrt{g_1 g_2} \lesssim 0.06 \frac{m_{k_2}}{\text{TeV}}. \quad (6)$$

Note that the scalar k_3 cannot be probed by τ decays at tree level. See Ref. [56] for the potential sensitivity of $\mu\text{TRISTAN}$.

We also consider constraints from leptonic anomalous magnetic dipole moments. The electromagnetic current of a lepton of mass m_ℓ is parametrised in terms of three form factors F_i for a real on-shell photon. In the CP conserving case, they reduce to the Dirac form factor F_1 and the Pauli form factor F_2 , see e.g. the discussion in [62, 69],

$$\langle \ell(\mathbf{p}_2) | j_{\text{em}}^\mu(0) | \ell(\mathbf{p}_1) \rangle = \bar{u}(\mathbf{p}_2) \left[F_1(q^2) \gamma^\mu + F_2(q^2) \frac{i\sigma^{\mu\nu}}{2m_\ell} q_\nu \right] u(\mathbf{p}_1) \quad \text{with} \quad p_1 = p_2 + q. \quad (7)$$

At $q^2 = 0$ the form factors are identified with the electric charge $F_1(0) = Q_\ell e$ and the anomalous magnetic moment $a_\ell = F_2(0)/F_1(0)$. We calculated the contribution of the doubly charged scalar to the anomalous magnetic moment using the general formulae in [53] and independently using FeynCalc [58, 71, 72, 73], FeynHelpers [70] and Package-X [65, 66]. The leading order contribution to the anomalous magnetic moment in an expansion in m_ℓ/m_k is given by

$$\Delta a_\ell = -\frac{(y^\dagger y)_{\ell\ell} m_\ell^2}{24\pi^2 m_k^2} \quad (8)$$

which agrees in magnitude with [54], but corrects the overall sign. It is also consistent with the result in [74].

There are two independent determinations of the electron anomalous magnetic moment, one using cesium [63] and the other rubidium [60] which result in the constraints

$$\Delta a_e^{\text{Cs}} = (-8.8 \pm 3.6) \times 10^{-13} \quad \Rightarrow \quad (y^\dagger y)_{ee}^{1/2} < 34[38] \frac{m_k}{\text{TeV}}, \quad (9)$$

$$\Delta a_e^{\text{Rb}} = (4.8 \pm 3.0) \times 10^{-13} \quad \Rightarrow \quad (y^\dagger y)_{ee}^{1/2} < [10] \frac{m_k}{\text{TeV}} \quad (10)$$

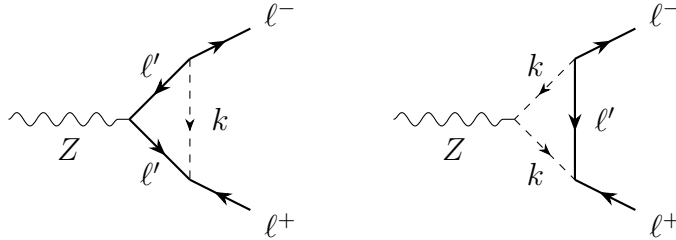


Figure 1: The doubly-charged scalar vertex corrections to $Z \rightarrow \ell^+\ell^-$. There are also self-energy corrections that we do not show. All corrections have been incorporated in the final result. The virtual lepton ℓ' may be of a different flavour from the final state leptons ℓ .

at $1[2]\sigma$. Due to the difference in sign of the predicted Δa_e in Eq. (8) and the central value of the rubidium measurement, the doubly charged isosinglet scalar is only compatible with the Δa_e measurement in rubidium at 2σ .

For the anomalous magnetic moment of the muon, we conservatively compare the experimental results [22, 7] with the theory prediction in the white paper [12], where the hadronic vacuum polarization has been replaced by the recent lattice result of the BMW collaboration [29, 28] following [14]. Demanding the deviation to be less than $1[2]\sigma$ we find

$$\Delta a_\mu = (4.0 \pm 4.4) \times 10^{-10} \quad \Rightarrow \quad (y^\dagger y)_{\mu\mu}^{1/2} < 0.92[3.2] \frac{m_k}{\text{TeV}}. \quad (11)$$

3. One-loop-induced processes: constraints and prospects

We now turn our attention to the main section of this paper: an analysis of constraints arising from 1-loop contributions to $Z \rightarrow \ell^+\ell^-$, $H \rightarrow \gamma\gamma$ and $H \rightarrow Z\gamma$ from existing data, and the determination of parameter-space reach at future colliders. We focus on flavour conserving Z boson decays but it is straightforward to generalise our results to flavour violating Z boson decays. Note that in the case of the triality models, that symmetry forbids CLFV violating $Z \rightarrow \ell^+\ell'^-$ decays.

3.1. $Z \rightarrow \ell^+\ell^-$

The Yukawa couplings y_{ij} in Eq. (1) modify the couplings of the Z boson to charged leptons at one loop level. Since the flavour conserving Z boson couplings have been measured very precisely at LEP and SLD, we expect that stringent constraints may arise. We show the one-loop vertex corrections due to k_i in Fig. 1.

To compute these corrections we write the tree plus one-loop vertex factor as

$$\Gamma_\mu^\ell = -2^{1/4} G_F^{1/2} m_Z \gamma_\mu [(g_R^\ell + \delta g_R^\ell) P_R + (g_L^\ell + \delta g_L^\ell) P_L] \quad (12)$$

where the tree-level SM values are $g_R^\ell = 2s_Z^2$ and $g_L^\ell = g_R^\ell - 1$ universally for $\ell = e, \mu, \tau$, with s_Z being the sine of the weak mixing angle in the renormalisation scheme we utilise. That scheme uses the precisely measured parameters G_F (from muon decay), m_Z and $\alpha(m_Z)$ as input, so

the definition of the weak mixing angle then becomes⁴

$$s_Z^2 c_Z^2 \equiv \frac{\pi \alpha(m_Z)}{\sqrt{2} G_F m_Z}. \quad (13)$$

The quantities δg_R^ℓ and δg_L^ℓ are the one-loop corrections induced by k interactions, and are discussed below.

To simplify our calculation we treat the leptons as massless, in which case there are no corrections to G_F . We also assume that the new scalar k is more massive than the Z -boson. There are two types of vertex corrections: the first one depends on the Yukawa couplings of the doubly charged scalars and is purely right-handed. It arises from the triangle diagrams and the lepton wave-function renormalisation. The second type of correction is common to all leptons arising from the renormalisation of α , m_Z , s_Z , the Z wave function renormalisation, and $Z - \gamma$ mixing. Some details of the calculation, including analytic expressions with the vertex dependence on the mass of k for $\delta g_R^{e,\mu,\tau}$ and $\delta g_L^{e,\mu,\tau}$ are presented in [Appendix A](#) for completeness.

With these ingredients we find for the doubly-charged isosinglet scalar that⁵

$$\delta g_R^\ell = (y^\dagger y)_{\ell\ell} \delta r_A(m_k) + \Delta r(m_k). \quad (14)$$

The left-handed Z -boson couplings are

$$\delta g_L^\ell = \Delta l(m_k) \quad (15)$$

with the explicit formula for $\Delta l(m_k)$ given in Eq. (A.3). Numerically, only the terms with $\delta r_A(m_k)$ are important when their corresponding coupling constants y are of order one.

For scalar masses $m_k \in [0.1, 5]$ TeV, the function δr_A ranges from 10^{-3} to 10^{-6} in magnitude. Current experiments are only sensitive to the real part of δg_R^ℓ , which interferes with the SM contribution. The real part of δg_R^ℓ is well approximated by

$$\text{Re}(\delta g_R^\ell) = (y^\dagger y)_{\ell\ell} \text{Re}(\delta r_A), \quad \text{Re}(\delta r_A) = 3.75 \times 10^{-5} \left(\frac{m_k}{1 \text{ TeV}} \right)^{-1.55}, \quad (16)$$

which is illustrated in Fig. 2.

The corrections from renormalisation that give rise to $\Delta r(m_k)$ and $\Delta l(m_k)$ affect many other observables as well and as such they should be constrained by a global fit. However, they are numerically insignificant, having values at most of the order of 10^{-6} for m_k in the regime of interest. A comparison with the values extracted from LEP plus SLD data assuming lepton universality [68],

$$g_A^\ell = -0.50123 \pm 0.00026, \quad g_V^\ell = -0.03783 \pm 0.00041, \quad (17)$$

⁴Details for the different ingredients that enter the calculation of these corrections in this scheme follow [38] closely.

⁵The generalization to lepton flavour violating Z boson decays is straightforward. The lepton-flavour violating right-handed Z -boson couplings are $\delta g_R^{ij} = (y^\dagger y)_{ij} \delta r_A(m_k) + \Delta r(m_k)$, where the first (second) index i (j) denotes the (anti-)lepton flavour in the final state.

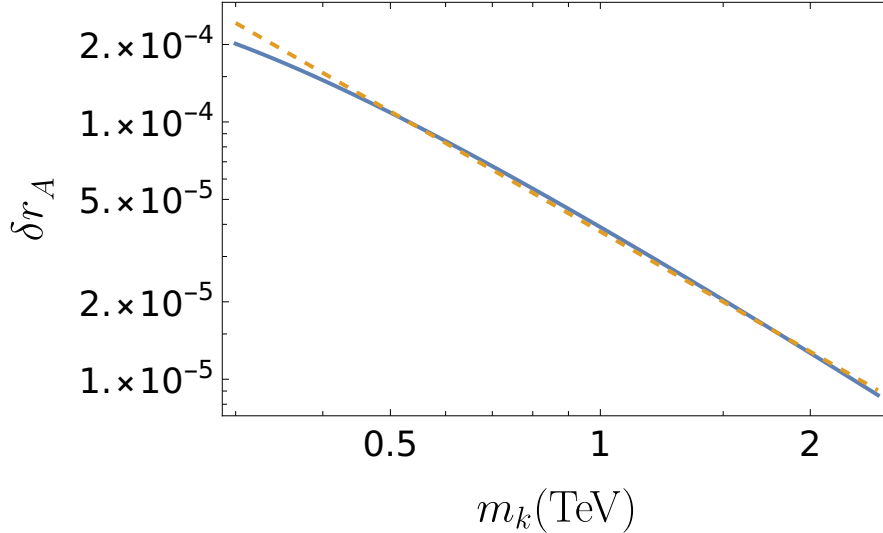


Figure 2: δr_A as a function of the scalar mass m_k . The dashed orange line shows the approximation in Eq. (16) to the full numerical result of δr_A (blue solid line).

confirms that these terms are indeed negligible for values of m_k above 300 GeV.⁶ Since the SM obeys lepton flavour universality, in the following analysis of the flavour universality violating effects we take the comparison best fit value to be given by Eq. (17).

To constrain the flavour universality violating terms proportional to one of the Yukawa coupling combinations $(y^\dagger y)_{\ell\ell}$, we add them to the SM contribution and compare with the values given by the combined LEP and SLD data without the assumption of lepton universality, namely [68]

$$\begin{aligned}
 g_L^e &= -0.26963 \pm 0.00030, & g_R^e &= 0.23148 \pm 0.00029, \\
 g_L^\mu &= -0.2689 \pm 0.0011, & g_R^\mu &= 0.2323 \pm 0.0013, \\
 g_L^\tau &= -0.26930 \pm 0.00058, & g_R^\tau &= 0.23274 \pm 0.00062.
 \end{aligned}
 \tag{18}$$

The results are illustrated in Fig. 3, where we include only the real parts of the effective couplings. The imaginary parts do not interfere with the leading order SM contribution and thus enter at a higher order. We have checked numerically that their effect is small. The oval contours show the 68% C.L. allowed regions corresponding to the combined LEP and SLD fit, with the lepton universal best fit point marked by the black star [68].⁷ The thin blue line extending from the star illustrates the corrections arising from the universality violating contributions. The physical meaning of this line depends on which coupling is considered. We have marked several parameter points on this line to illustrate the sensitivity for different couplings y and doubly-charged scalar masses m_k . The figure shows that switching on the doubly-charged scalar Yukawa couplings tends to worsen the fit to the e^+e^- data but improve the fit to the $\tau^+\tau^-$ data. We emphasise that while there is no significant tension between the

⁶Note that $g_A = (g_L - g_R)/2$ and $g_V = (g_L + g_R)/2$.

⁷Note that the oval contours account for correlations, unlike the ranges quoted in Eq. (18).

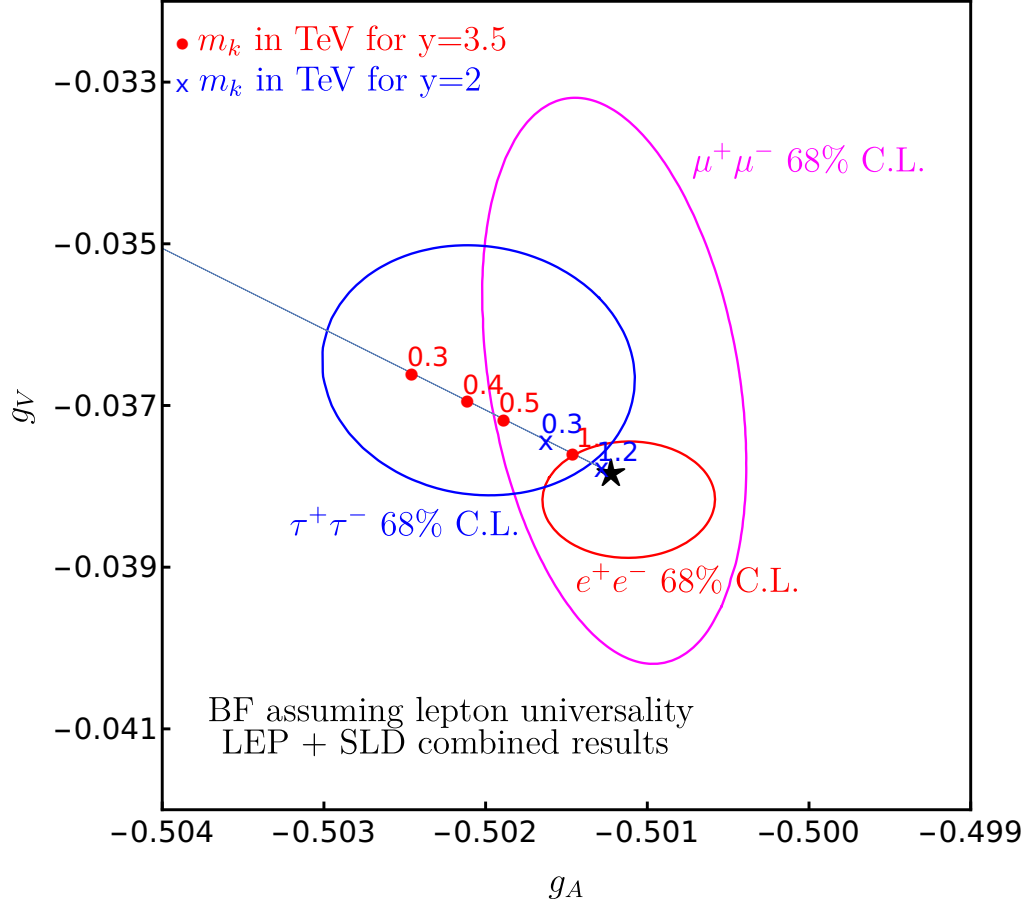


Figure 3: LEP plus SLD allowed regions shown as the ellipse contours at 68% C.L.. The black star is the lepton universal best fit (BF) point [68]. Lepton flavour universality violating corrections to $Z\ell\ell$ shown by the thin blue line. The real parts of g_A and g_V are plotted. Blue crosses (red circles) along this line mark illustrative values of m_k in TeV for $y = 2$ ($y = 3.5$). The coupling constant y in this case generically refers to $y \equiv \sqrt{(y^\dagger y)\ell\ell}$ which appears in Eq. (14).

data in the three channels and the SM, the doubly-charged scalar Yukawa couplings produce an interesting flavour-dependent effect with a systematic trend.

Future colliders will provide improved sensitivity to the leptonic Z -boson couplings. We now consider the sensitivity of four future colliders, with parameters extracted from Ref. [27]: the HL-LHC [32] with integrated luminosity of 6 ab^{-1} in 12 years; the ILC at 250 GeV with 2 ab^{-1} ; CEPC over 10 years for three different centre-of-mass energies: $\sqrt{s} = m_Z$ (60 ab^{-1}), $\sqrt{s} = 2m_W$ (3.6 ab^{-1}), and 240 GeV (12 ab^{-1}); and the Future Circular Collider in the electron-positron configuration (FCC-ee) with runs at centre-of-mass energies m_Z (150 ab^{-1}), $2m_W$ (10 ab^{-1}), 240 GeV (5 ab^{-1}) and 365 GeV (1.5 ab^{-1}) over a period of 13 years. This will amount to 5×10^{12} Z bosons, an improvement of more than five orders of magnitude over LEP which

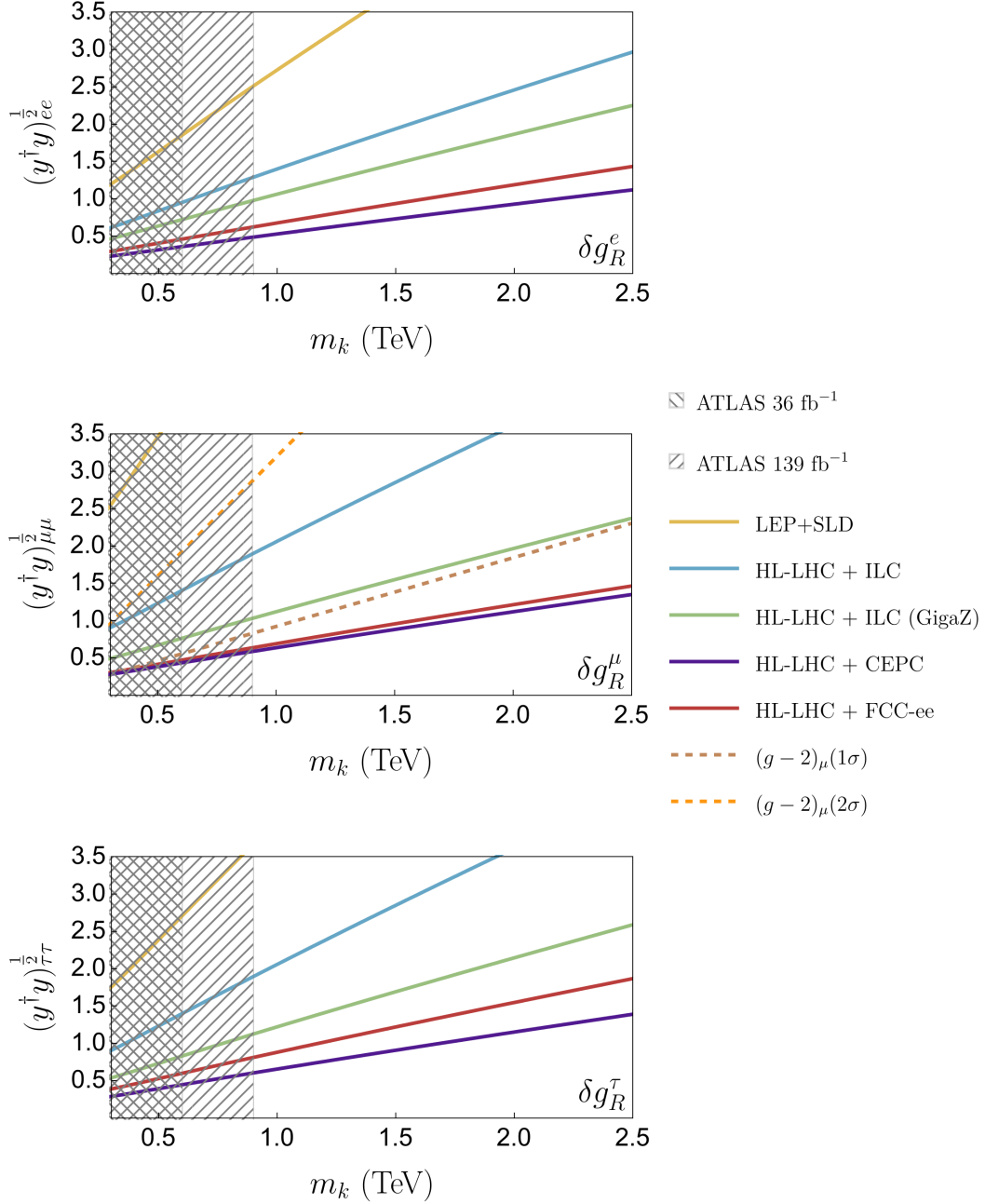


Figure 4: Constraints and parameter-space reach for the leptonic Z boson couplings δg_R^ℓ , with $\ell = e, \mu, \tau$. According to Eqs. (19) to (21), for the $T = (1, 2, 3)$ model, δg_R^e varies with (f_2, g_1, h_1) respectively, δg_R^μ varies with (f_1, g_2, h_1) , and δg_R^τ varies with (f_1, g_1, h_2) . The mass of the doubly charged scalar m_k is constrained by direct searches at the LHC to be larger than 600 GeV (ATLAS 36 fb⁻¹), or 900 GeV for universal lepton couplings (ATLAS 139 fb⁻¹), as discussed in Sec. 2.3 and shown by the grey hatched regions. The region below the yellow contour corresponds to the allowed parameter space from the existing LEP and SLD bounds, with the uncertainty at the 61% level [68]. The large improvement in sensitivity at the future colliders HL-LHC combined with ILC, ILC (Giga-Z), CEPC, and FCC-ee is illustrated by the blue, green, purple, and red lines, respectively; the uncertainties are at the 1 σ level.

	LEP+SLD	ILC +HL-LHC	ILC (Giga Z) +HL-LHC	CEPC +HL-LHC	FCC-ee +HL-LHC
δg_R^e [$\times 10^4$]	2.9	0.76	0.44	0.11	0.18
δg_R^μ [$\times 10^4$]	13.0	1.64	0.48	0.16	0.18
δg_R^τ [$\times 10^4$]	6.2	1.65	0.58	0.17	0.30

Table 1: Existing or expected experimental precision for the leptonic Z -boson gauge couplings (multiplied by 10^4). The existing experimental uncertainty for LEP+SLD was taken from Table 7.7 in Ref. [68] while the sensitivities for the combination of the future lepton colliders with the HL-LHC have been extracted from Figure 8 in Ref. [21]. Giga Z refers to a Z pole run, i.e. $\sqrt{s} = m_Z$, at the ILC. The uncertainty of LEP+SLD is at the 61% level [68] and the future sensitivities are at the 1σ level. Note that despite the large increase in statistics, the improved reach expected at the future colliders is limited by systematic uncertainties – see e.g. Ref. [27].

recorded 1.7×10^7 Z bosons [68].⁸ Moreover, a $\sqrt{s} = m_Z$ Z -pole run called “Giga Z” is possible at the ILC which would drastically improve the experimental sensitivity. We analyse this for an integrated luminosity of 100 fb^{-1} over a period of 1 to 3 years.

Figure 4 shows the relevant parameter space region for the Yukawa coupling combination $(y^\dagger y)_{\ell\ell}^{1/2}$ as a function of the doubly-charged scalar mass m_k . It uses the experimental uncertainties on the leptonic Z boson couplings $\delta g_R^{e,\mu,\tau}$ given in Table 1 to either constrain doubly-charged scalar boson parameter space (existing LEP+SLD data) or show the expected sensitivity of the combination of HL-LHC and the other future colliders we are considering. These results are derived from Eq. (14) noting $\Delta r(m_k)$ is negligible. The experimental uncertainties for the current best measurements from LEP+SLD have been taken from Table 7.7 in [68] (as also quoted in Eq. (18)) and the sensitivities of the future lepton colliders combined with the HL-LHC are extracted from Figure 8 in Ref. [21].⁹ The yellow contour is the upper edge of the currently allowed parameter space from LEP+SLD data, while the blue, green, purple and red lines are projections for the lower edge of the parameter reach of the HL-LHC combined with ILC, ILC (Giga-Z), CEPC and FCC-ee respectively. The constraints are approximately proportional to $m_k^{0.775}$, which originates from the functional form of δr_A , see Eq. (16). For comparison we also include the constraint from the muon anomalous magnetic moment measurement as dashed lines. It is stronger than the current LEP+SLD bound and even outperforms the combination of HL-LHC with the ILC (GigaZ). The electron anomalous magnetic moment measurements are currently not competitive. The approximate exclusion limits from direct searches at ATLAS are indicated by the hatched regions, with labels of “ATLAS 36 fb^{-1} ” and “ATLAS 139 fb^{-1} ” as per the discussion in Sec. 2.2.

⁸SLD produced 6×10^5 Z bosons.

⁹Note the different definitions of the parameters δg . While we use the absolute uncertainty, Ref. [21] uses a relative uncertainty.

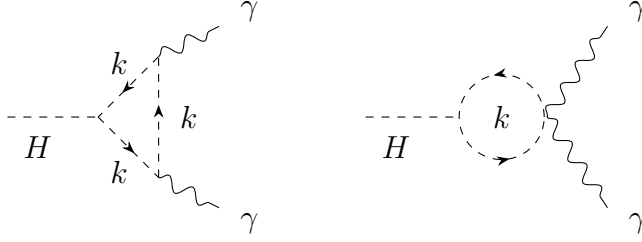


Figure 5: The doubly-charged scalar contributions to $H \rightarrow \gamma\gamma$.

The results straightforwardly translate to the lepton triality models. The corrections to the right-handed Z -boson couplings can be explicitly written as

$$\delta g_R^{\mu,\tau} = f_1^2 \delta r_A(m_{k_1}) + \Delta r(m_{k_1}), \quad \delta g_R^e = f_2^2 \delta r_A(m_{k_1}) + \Delta r(m_{k_1}), \quad (19)$$

in the $T = 1$ model, whereas for the $T = 2$ model we have that

$$\delta g_R^{e,\tau} = g_1^2 \delta r_A(m_{k_2}) + \Delta r(m_{k_2}), \quad \delta g_R^\mu = g_2^2 \delta r_A(m_{k_2}) + \Delta r(m_{k_2}), \quad (20)$$

and for the $T = 3$ model,

$$\delta g_R^{e,\mu} = h_1^2 \delta r_A(m_{k_3}) + \Delta r(m_{k_3}), \quad \delta g_R^\tau = h_2^2 \delta r_A(m_{k_3}) + \Delta r(m_{k_3}). \quad (21)$$

Hence δg_R^e varies with (f_2, g_1, h_1) , δg_R^μ varies with (f_1, g_2, h_1) and δg_R^τ varies with (f_1, g_1, h_2) .

3.2. $H \rightarrow \gamma\gamma$ and $H \rightarrow Z\gamma$

We now return to the general model. After electroweak symmetry breaking, the Higgs portal coupling produces a cubic interaction between the physical Higgs boson and the doubly charged scalar:

$$\kappa_\phi \phi^\dagger \phi |k|^2 \supset \kappa_\phi v H |k|^2 \quad (22)$$

where $\phi^0 = (v + H)/\sqrt{2}$ in unitary gauge. This interaction produces a BSM contribution to the two-photon decay of the Higgs boson from doubly-charged scalar loops, with the vertex corrections shown in Fig. 5. Relative to the SM the $H \rightarrow \gamma\gamma$ rate becomes,

$$R_{\gamma\gamma} = \frac{\Gamma(H \rightarrow \gamma\gamma)}{\Gamma(H \rightarrow \gamma\gamma)_{SM}} = \left| \frac{I_V(\tau_W) + \frac{4}{3}I_q(\tau_t) + 2\kappa_\phi \frac{v^2}{m_{k_i}^2} I_S(\tau_k)}{I_V(\tau_W) + \frac{4}{3}I_q(\tau_t)} \right|^2 \quad (23)$$

where I_V and I_q are the well-known loop factors for the W and t -quark SM contributions, and I_S is the corresponding loop function for the new contribution due to the k scalar. The arguments are given by $\tau_a = 4m_a^2/m_H^2$ where $a = W, t, k$, with m_H being the mass of the Higgs boson. The loop functions are collected in [Appendix B](#) for reference. This result agrees with Ref. [37] when the latter is specialised to couplings pertaining to our model.

In the top panel of Fig. 6 the yellow-shaded area shows the region of $m_k - \kappa_\phi$ parameter space that is currently allowed at 1σ by the ATLAS Run 2 measurements, $R_{\gamma\gamma} = 1.088_{-0.09}^{+0.095}$

[15], assuming no new physics in the production process. We show values of κ_ϕ in the range $[-1.8, 10]$ which are consistent with perturbative unitarity and the bounded-from-below bounds discussed in Sec. 2. Note that the current measurements favour BSM contributions that increase the rate compared to the SM, whereas in general BSM can also reduce the rate. This occurs for negative values of κ_ϕ in our models.

In the lower panel of Fig. 6 we show the expected sensitivities of the future colliders using parameters extracted from Table 6 in Ref. [39]. The region bounded by the orange contour illustrates the future sensitivity of HL-LHC, derived from the expected precision $\Delta\kappa_\gamma = 1.8\%$ where $R_{\gamma\gamma} = \kappa_\gamma^2$. The blue line illustrates the sensitivity of an e^+e^- collider combined with HL-LHC, where we suppose a centre-of-mass energy of 240 GeV and 5 ab^{-1} of data, which leads to $\Delta\kappa_\gamma = 1.3\%$, corresponding to the FCC-ee sensitivity. However, similar results may be achieved by CEPC ($\Delta\kappa_\gamma = 1.68\%$) and ILC ($\Delta\kappa_\gamma = 1.36\%$) with the same centre-of-mass energy of 240 GeV; both are also combined with HL-LHC. A single line thus suffices to illustrate all proposed e^+e^- colliders. Finally, the green contour pertains to the full integrated FCC program (ee , eh and hh) with $\Delta\kappa_\gamma = 0.29\%$. Note that FCC-int is not combined with HL-LHC. A detailed discussion of the luminosities for each run of the FCC, CEPC and ILC programs are described in Sec. 3.1.

Following a very similar procedure to the above, we can write for the $H \rightarrow Z\gamma$ decay that

$$R_{Z\gamma} = \frac{\Gamma(H \rightarrow Z\gamma)}{\Gamma(H \rightarrow Z\gamma)_{SM}} = \left| \frac{A_t^{Z\gamma} + A_W^{Z\gamma} + A_k^{Z\gamma}}{A_t^{Z\gamma} + A_W^{Z\gamma}} \right|^2 \quad (24)$$

where

$$A_t^{Z\gamma} = \frac{-4(\frac{1}{2} - \frac{4}{3} \sin^2 \theta_W)}{\sin \theta_W \cos \theta_W} [I_1(\tau_t, \lambda_t) - I_2(\tau_t, \lambda_t)], \quad (25a)$$

$$A_W^{Z\gamma} = -\cot \theta_W \left[4(3 - \tan^2 \theta_W) I_2(\tau_W, \lambda_W) + \left[(1 + \frac{2}{\tau_W}) \tan^2 \theta_W - (5 + \frac{2}{\tau_W}) \right] I_1(\tau_W, \lambda_W) \right], \quad (25b)$$

$$A_k^{Z\gamma} = -4\kappa_\phi \tan \theta_W \frac{v^2}{m_k^2} I_1(\tau_k, \lambda_k), \quad (25c)$$

with $\lambda_a = 4m_a^2/m_Z^2$, and with the known one-loop functions I_1 and I_2 given in Appendix C for reference. The SM top-quark and W -boson contributions ($A_t^{Z\gamma}$, $A_W^{Z\gamma}$) have been first calculated in Ref. [23] and are taken from Ref. [44] and the scalar contribution is similar to that of the physical charged Higgs boson in two-Higgs-doublet models. The vertex corrections induced by k interactions are shown in Fig. 7.

The ratio $R_{Z\gamma} = 2.2 \pm 0.7$ has been recently measured [15, 2]¹⁰, and the future precision at HL-LHC is expected to be $\Delta\kappa_{Z\gamma} = 9.8\%$ where $R_{Z\gamma} = \kappa_{Z\gamma}^2$ [27, 36, 16, 59]. Future lepton colliders cannot improve this measurement. The full FCC program with $ee/eh/hh$ running would,

¹⁰We do not attempt to explain the hint of an excess over the SM expectation – see Refs. [30, 51, 48] for possible explanations.

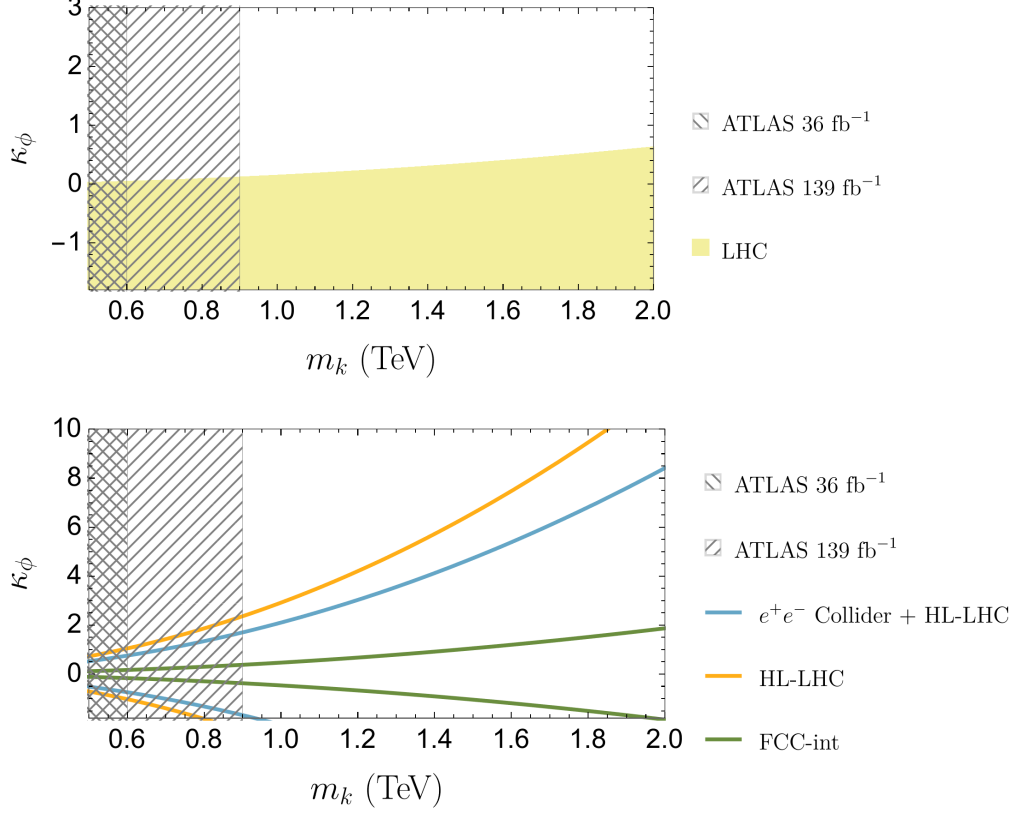


Figure 6: Experimental sensitivity to the Higgs portal coupling κ_ϕ from precise measurements of $H \rightarrow \gamma\gamma$ as a function of m_k . Both panels show the current ATLAS indicative constraints from direct searches as exclusion regions in grey hatch. The yellow region in the top panel shows the currently allowed region from the Higgs diphoton channel. The lower panel shows the projections for HL-LHC with 6 ab^{-1} of data in orange, a future e^+e^- collider running at 240 GeV taking 5 ab^{-1} of data in blue combined with HL-LHC (see text for discussion), and the integrated FCC program (ee , eh and hh) in green. The colliders are able to probe the regions outside the contours.

however, increase the precision to $\Delta\kappa_{Z\gamma} = 0.69\%$ [27, 24]. Since this observable is currently measured less precisely than $R_{\gamma\gamma}$, and that situation is expected to continue into the future, it is not expected to provide competitive constraints on the parameter space. Nevertheless, it is interesting to quantify the effect of the BSM physics we are considering, which is done in Fig. 8. We see that deviations from the SM would be at most at the 31–33% level in $H \rightarrow Z\gamma$ compared to $H \rightarrow \gamma\gamma$. To understand the plot properly, note that in the limit $m_k \rightarrow \infty$, where the new physics decouples, this ratio goes to one-loop accuracy as:¹¹

$$\frac{R_{Z\gamma} - 1}{R_{\gamma\gamma} - 1} \approx -\tan\theta_W \left(1 + \frac{1}{15} \frac{m_Z^2}{m_k^2}\right) \sqrt{1 - \frac{m_Z^2}{m_h^2}} \sqrt{\frac{\mathcal{B}(h \rightarrow \gamma\gamma)_{SM}}{\mathcal{B}(h \rightarrow Z\gamma)_{SM}}}. \quad (26)$$

¹¹Note that higher-order corrections are important in the SM. The ratio of branching ratios $\sqrt{\frac{\mathcal{B}(h \rightarrow \gamma\gamma)_{SM}}{\mathcal{B}(h \rightarrow Z\gamma)_{SM}}} = 0.824$ [41] receives a $\sim 45\%$ correction over the leading-order (one-loop) prediction of 0.570.

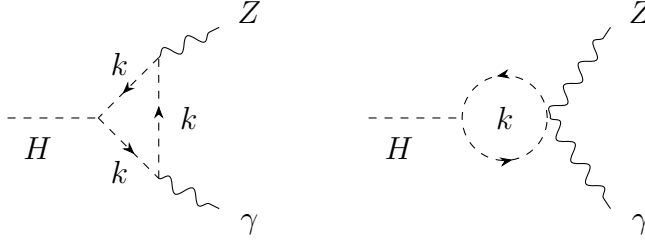


Figure 7: The doubly-charged scalar contributions to $H \rightarrow Z\gamma$. We do not show the self-energy corrections, but they are incorporated in the final result.

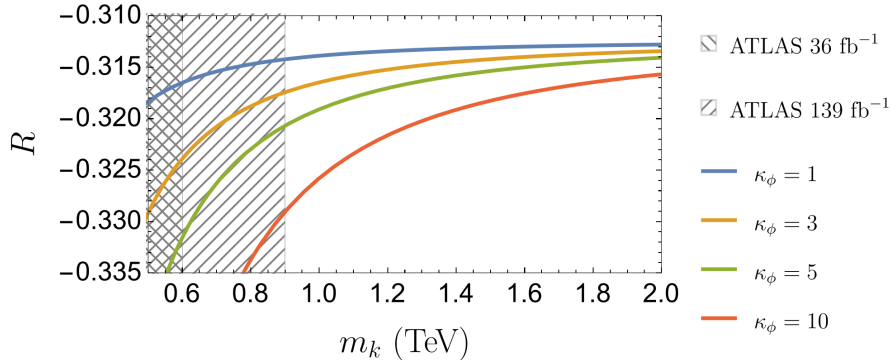


Figure 8: The ratio $R = (R_{Z\gamma} - 1)/(R_{\gamma\gamma} - 1)$ as a function of m_{k_i} for selected values of κ_ϕ . This demonstrates that $H \rightarrow Z\gamma$ is at best about an order of magnitude less sensitive to doubly-charged scalar loop effects compared to $H \rightarrow \gamma\gamma$.

The anticipated $\Delta\kappa_{Z\gamma} = 9.8\%$ precision at HL-LHC will not be sufficient to constrain the (m_{k_i}, κ_ϕ) parameter space in any meaningful way. Figure 9 shows the constraints that could be achieved with hypothetical precision measurements at the $\Delta\kappa_{Z\gamma} = 3\%$, 1.5% and 0.69% levels.

The results directly apply to the lepton triality models, because the Higgs portal coupling κ is not affected by the lepton triality symmetry.

4. Conclusion

We revisited corrections to the leptonic Z -boson couplings and Higgs boson decays to two photons or a photon and a Z boson in models with a doubly-charged scalar k . These general results have then been applied to simple lepton triality models featuring doubly-charged scalar bosons k_i which serve as useful benchmark BSM scenarios for charged lepton flavour violation.

Precision measurements of the leptonic Z -boson couplings are sensitive to both flavour-preserving and flavour-changing Yukawa couplings of the doubly-charged scalar. We have found that the processes $Z \rightarrow \ell^+\ell^-$ ($\ell = e, \mu, \tau$), which conserve lepton flavour, exhibit interesting flavour non-universality effects due to one-loop level interactions of the doubly-charged scalar, as summarised in Figs. 3 and 4. Figure 3 shows that doubly-charged scalars can improve the fit to the $Z\tau\tau$ coupling but at the expense of the Zee coupling. Figure 4 shows both existing bounds from LEP+SLD and the future parameter-space reach of HL-LHC when combined,

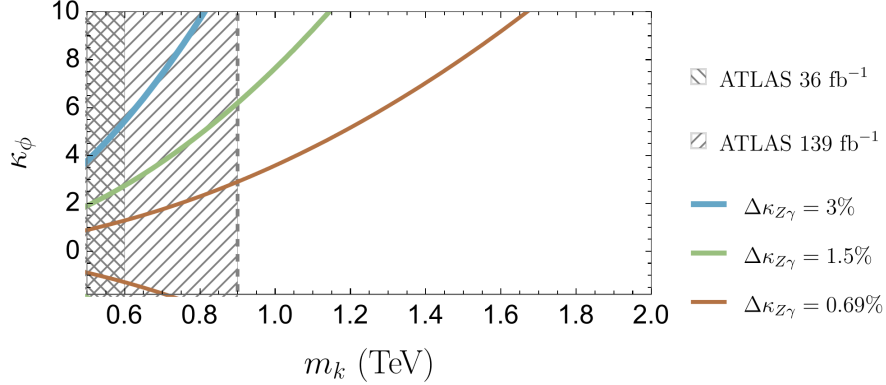


Figure 9: The anticipated HL-LHC precision of $\Delta\kappa_{Z\gamma} = 9.8\%$ for $R_{Z\gamma}$ will be insufficient to constrain the (m_k, κ_ϕ) parameter space in any meaningful way. The curves show the parameter space that could be probed by hypothetical precision measurements at the $\Delta\kappa_{Z\gamma} = 3\%$, 1.5% and 0.69% . These regions lie outside the blue, green and brown curves, respectively. The integrated FCC (ee , eh and hh) is expected to reach a $\Delta\kappa_{Z\gamma} = 0.69\%$ sensitivity [24].

respectively, with the ILC, ILC (Giga Z), CEPC, and FCC-ee which can be directly applied to the lepton triality specific cases.

In addition, the Higgs portal coupling κ_ϕ between the doubly-charged scalar k and the standard Higgs boson is constrained, as a function of m_k , by $H \rightarrow \gamma\gamma$, as depicted in Fig. 6. This figure also shows the future sensitivity at the HL-LHC and future e^+e^- colliders. Effects on $H \rightarrow Z\gamma$ were also analysed, but this decay mode is not expected to provide useful constraints for the foreseeable future.

Acknowledgments

We thank Fang Xu for communication about the anomalous magnetic moment. This work was supported in part by Australian Research Council Discovery Project DP200101470.

Appendix A. $Z \rightarrow \ell^+\ell^-$

To obtain these results we have implemented the model in `FeynRules` [34, 8] to generate `FeynArts` [45] output where `LoopTools` [46] is used to compute the one-loop diagrams and simplification is assisted with `FeynCalc` [58, 71, 72, 73], `FeynHelpers` [70] and `Package-X` [65, 66].

We combine the different ingredients of the calculation to obtain,

$$\delta r_A(m_k) = \frac{s_Z^2}{32\pi^2 m_Z^2} \left(-4m_k^4 (C_0(0, 0, m_Z^2, 0, m_k^2, 0) + 2C_0(0, 0, m_Z^2, m_k^2, 0, m_k^2)) \right. \\ \left. + 4 \frac{2m_k^2 - m_Z^2}{m_Z} \mathcal{H}(m_k, m_Z) - 7m_Z^2 + 2(2m_k^2 - m_Z^2)(1 - i\pi - 2 \log(m_k/m_Z)) \right), \quad (\text{A.1})$$

$$\Delta r(m_k) = \frac{e^2 s_Z^2}{36\pi^2 c_Z^2 (c_Z^2 - s_Z^2)} \frac{1}{m_Z^3} \left(6(\mathcal{H}(m_k, m_Z) + 2m_Z)((3s_Z^4 - 3s_Z^2 c_Z^2 + 4c_Z^4)m_k^2 - c_Z^4 m_Z^2) \right. \\ \left. - m_Z^3(3s_Z^4 - 3s_Z^2 c_Z^2 + 4c_Z^4) \right), \quad (\text{A.2})$$

$$\Delta l(m_k) = \frac{e^2 s_Z^2}{36\pi^2 c_Z^2 (c_Z^2 - s_Z^2)} \frac{1}{m_Z^3} \left(6(\mathcal{H}(m_k, m_Z) + 2m_Z)((3s_Z^4 - 3s_Z^2 c_Z^2 + 4c_Z^4)m_k^2 - c_Z^4 m_Z^2) \right. \\ \left. - m_Z^3(3s_Z^4 - 3s_Z^2 c_Z^2 + 4c_Z^4) + (c_Z^2 - s_Z^2)(9m_k^2(\mathcal{H}(m_k, m_Z) + 2m_Z) - \frac{3}{2}m_Z^3) \right). \quad (\text{A.3})$$

We have left our result in terms of the Passarino-Veltman function C_0 for compactness. The complete vertex corrections are constructed from these functions as in Eq. (14). The loop function \mathcal{H} , can be written in terms of

$$r^2 = \frac{m_Z^2}{4m_k^2} \quad (\text{A.4})$$

for $r \leq 1$ as

$$\mathcal{H}(m_k, m_Z) = -m_Z \frac{1}{r} \sqrt{1 - r^2} \arccos(1 - 2r^2). \quad (\text{A.5})$$

Appendix B. $H \rightarrow \gamma\gamma$

For convenience we list here the standard one-loop form factors that appear in $H \rightarrow \gamma\gamma$ for intermediate vectors, fermions and scalars, respectively:

$$\begin{aligned} I_V(x) &= 2 + 3x + 3x(2 - x)\mathcal{F}(x), \\ I_F(x) &= -2x(1 + (1 - x)\mathcal{F}(x)), \\ I_S(x) &= x(1 - x\mathcal{F}(x)), \end{aligned} \quad (\text{B.1})$$

where

$$\mathcal{F}(x) = \begin{cases} -\frac{1}{4} \left(\ln \left(\frac{1 + \sqrt{1-x}}{1 - \sqrt{1-x}} \right) - i\pi \right)^2 & \text{for } x < 1 \\ \left(\arcsin \sqrt{\frac{1}{x}} \right)^2 & \text{for } x \geq 1 \end{cases}. \quad (\text{B.2})$$

Appendix C. $H \rightarrow Z\gamma$

The one-loop form factors in this case are

$$I_1(x, y) = \frac{xy}{2(x-y)} + \frac{x^2y^2}{2(x-y)^2}[\mathcal{F}(x) - \mathcal{F}(y)] + \frac{x^2y}{(x-y)^2}[\mathcal{G}(x) - \mathcal{G}(y)], \quad (\text{C.1})$$

$$I_2(x, y) = -\frac{xy}{2(x-y)}[\mathcal{F}(x) - \mathcal{F}(y)], \quad (\text{C.2})$$

where

$$\mathcal{G}(x) = \begin{cases} \frac{1}{2}\sqrt{1-x} \left(\ln \left(\frac{1+\sqrt{1-x}}{1-\sqrt{1-x}} \right) - i\pi \right) & \text{for } x < 1 \\ \sqrt{x-1} \arcsin \sqrt{\frac{1}{x}} & \text{for } x \geq 1 \end{cases}. \quad (\text{C.3})$$

References

- [1] Aaboud, M., et al. (ATLAS), 2018. Search for doubly charged Higgs boson production in multi-lepton final states with the ATLAS detector using proton–proton collisions at $\sqrt{s} = 13$ TeV. *Eur. Phys. J. C* 78, 199. doi:[10.1140/epjc/s10052-018-5661-z](https://doi.org/10.1140/epjc/s10052-018-5661-z), [arXiv:1710.09748](https://arxiv.org/abs/1710.09748).
- [2] Aad, G., et al. (CMS, ATLAS), 2023a. Evidence for the Higgs boson decay to a Z boson and a photon at the LHC. [arXiv:2309.03501](https://arxiv.org/abs/2309.03501).
- [3] Aad, G., et al. (ATLAS), 2023b. Search for doubly charged Higgs boson production in multi-lepton final states using 139 fb^{-1} of proton–proton collisions at $\sqrt{s} = 13$ TeV with the ATLAS detector. *Eur. Phys. J. C* 83, 605. doi:[10.1140/epjc/s10052-023-11578-9](https://doi.org/10.1140/epjc/s10052-023-11578-9), [arXiv:2211.07505](https://arxiv.org/abs/2211.07505).
- [4] Abada, A., et al. (FCC), 2019. FCC Physics Opportunities: Future Circular Collider Conceptual Design Report Volume 1. *Eur. Phys. J. C* 79, 474. doi:[10.1140/epjc/s10052-019-6904-3](https://doi.org/10.1140/epjc/s10052-019-6904-3).
- [5] de Adelhart Toorop, R., Bazzocchi, F., Merlo, L., Paris, A., 2011a. Constraining Flavour Symmetries At The EW Scale I: The A4 Higgs Potential. *JHEP* 03, 035. doi:[10.1007/JHEP03\(2011\)035](https://doi.org/10.1007/JHEP03(2011)035), [arXiv:1012.1791](https://arxiv.org/abs/1012.1791). [Erratum: *JHEP* 01, 098 (2013)].
- [6] de Adelhart Toorop, R., Bazzocchi, F., Merlo, L., Paris, A., 2011b. Constraining Flavour Symmetries At The EW Scale II: The Fermion Processes. *JHEP* 03, 040. doi:[10.1007/JHEP03\(2011\)040](https://doi.org/10.1007/JHEP03(2011)040), [arXiv:1012.2091](https://arxiv.org/abs/1012.2091).
- [7] Aguillard, D.P., et al. (Muon g-2), 2023. Measurement of the Positive Muon Anomalous Magnetic Moment to 0.20 ppm. *Phys. Rev. Lett.* 131, 161802. doi:[10.1103/PhysRevLett.131.161802](https://doi.org/10.1103/PhysRevLett.131.161802), [arXiv:2308.06230](https://arxiv.org/abs/2308.06230).

- [8] Alloul, A., Christensen, N.D., Degrande, C., Duhr, C., Fuks, B., 2014. FeynRules 2.0 - A complete toolbox for tree-level phenomenology. *Comput. Phys. Commun.* 185, 2250–2300. doi:[10.1016/j.cpc.2014.04.012](https://doi.org/10.1016/j.cpc.2014.04.012), [arXiv:1310.1921](https://arxiv.org/abs/1310.1921).
- [9] Altarelli, G., Feruglio, F., 2006. Tri-bimaximal neutrino mixing, $A(4)$ and the modular symmetry. *Nucl. Phys. B* 741, 215–235. doi:[10.1016/j.nuclphysb.2006.02.015](https://doi.org/10.1016/j.nuclphysb.2006.02.015), [arXiv:hep-ph/0512103](https://arxiv.org/abs/hep-ph/0512103).
- [10] Anisha, Banerjee, U., Chakraborty, J., Englert, C., Spannowsky, M., Stylianou, P., 2022. Effective connections of $a\mu$, Higgs physics, and the collider frontier. *Phys. Rev. D* 105, 016019. doi:[10.1103/PhysRevD.105.016019](https://doi.org/10.1103/PhysRevD.105.016019), [arXiv:2108.07683](https://arxiv.org/abs/2108.07683).
- [11] Anisha, Das Bakshi, S., Banerjee, S., Biekötter, A., Chakraborty, J., Kumar Patra, S., Spannowsky, M., 2023. Effective limits on single scalar extensions in the light of recent LHC data. *Phys. Rev. D* 107, 055028. doi:[10.1103/PhysRevD.107.055028](https://doi.org/10.1103/PhysRevD.107.055028), [arXiv:2111.05876](https://arxiv.org/abs/2111.05876).
- [12] Aoyama, T., et al., 2020. The anomalous magnetic moment of the muon in the Standard Model. *Phys. Rept.* 887, 1–166. doi:[10.1016/j.physrep.2020.07.006](https://doi.org/10.1016/j.physrep.2020.07.006), [arXiv:2006.04822](https://arxiv.org/abs/2006.04822).
- [13] Aryshev, A., et al. (ILC International Development Team), 2022. The International Linear Collider: Report to Snowmass 2021 [arXiv:2203.07622](https://arxiv.org/abs/2203.07622).
- [14] Athron, P., Crivellin, A., Gonzalo, T.E., Iguro, S., Sierra, C., 2024. Global fit to the 2HDM with generic sources of flavour violation using GAMBIT [arXiv:2410.10493](https://arxiv.org/abs/2410.10493).
- [15] ATLAS collaboration, 2022a. A detailed map of Higgs boson interactions by the ATLAS experiment ten years after the discovery. *Nature* 607, 52–59. doi:[10.1038/s41586-022-04893-w](https://doi.org/10.1038/s41586-022-04893-w), [arXiv:2207.00092](https://arxiv.org/abs/2207.00092). [Erratum: *Nature* 612, E24 (2022)].
- [16] ATLAS collaboration, 2022b. Snowmass White Paper Contribution: Physics with the Phase-2 ATLAS and CMS Detectors. Technical Report. CERN. Geneva. URL: <https://cds.cern.ch/record/2805993>. all figures including auxiliary figures are available at <https://atlas.web.cern.ch/Atlas/GROUPS/PHYSICS/PUBNOTES/ATL-PHYS-PUB-2022-018>.
- [17] Babu, K.S., 1988. Model of 'Calculable' Majorana Neutrino Masses. *Phys. Lett. B* 203, 132–136. doi:[10.1016/0370-2693\(88\)91584-5](https://doi.org/10.1016/0370-2693(88)91584-5).
- [18] Babu, K.S., Jana, S., 2017. Probing Doubly Charged Higgs Bosons at the LHC through Photon Initiated Processes. *Phys. Rev. D* 95, 055020. doi:[10.1103/PhysRevD.95.055020](https://doi.org/10.1103/PhysRevD.95.055020), [arXiv:1612.09224](https://arxiv.org/abs/1612.09224).
- [19] Baer, H., et al. (ILC), 2013. The International Linear Collider Technical Design Report - Volume 2: Physics. [arXiv:1306.6352](https://arxiv.org/abs/1306.6352).

- [20] Bambade, P., et al., 2019. The International Linear Collider: A Global Project [arXiv:1903.01629](#).
- [21] Belloni, A., et al., 2022. Report of the Topical Group on Electroweak Precision Physics and Constraining New Physics for Snowmass 2021 [arXiv:2209.08078](#).
- [22] Bennett, G.W., et al. (Muon g-2), 2006. Final Report of the Muon E821 Anomalous Magnetic Moment Measurement at BNL. *Phys. Rev. D* 73, 072003. doi:[10.1103/PhysRevD.73.072003](#), [arXiv:hep-ex/0602035](#).
- [23] Bergstrom, L., Hulth, G., 1985. Induced Higgs Couplings to Neutral Bosons in e^+e^- Collisions. *Nucl. Phys. B* 259, 137–155. doi:[10.1016/0550-3213\(85\)90302-5](#). [Erratum: *Nucl.Phys.B* 276, 744–744 (1986)].
- [24] Bernardi, G., et al., 2022. The Future Circular Collider: a Summary for the US 2021 Snowmass Process [arXiv:2203.06520](#).
- [25] Bigaran, I., He, X.G., Schmidt, M.A., Valencia, G., Volkas, R., 2023. Lepton-flavor-violating tau decays from triality. *Phys. Rev. D* 107, 055001. doi:[10.1103/PhysRevD.107.055001](#), [arXiv:2212.09760](#).
- [26] de Blas, J., Chala, M., Perez-Victoria, M., Santiago, J., 2015. Observable Effects of General New Scalar Particles. *JHEP* 04, 078. doi:[10.1007/JHEP04\(2015\)078](#), [arXiv:1412.8480](#).
- [27] de Blas, J., et al., 2020. Higgs Boson Studies at Future Particle Colliders. *JHEP* 01, 139. doi:[10.1007/JHEP01\(2020\)139](#), [arXiv:1905.03764](#).
- [28] Boccaletti, A., et al., 2024. High precision calculation of the hadronic vacuum polarisation contribution to the muon anomaly [arXiv:2407.10913](#).
- [29] Borsanyi, S., et al., 2021. Leading hadronic contribution to the muon magnetic moment from lattice QCD. *Nature* 593, 51–55. doi:[10.1038/s41586-021-03418-1](#), [arXiv:2002.12347](#).
- [30] Boto, R., Das, D., Romao, J.C., Saha, I., Silva, J.P., 2024. New physics interpretations for nonstandard values of $h \rightarrow Z\gamma$. *Phys. Rev. D* 109, 095002. doi:[10.1103/PhysRevD.109.095002](#), [arXiv:2312.13050](#).
- [31] Cao, Q.H., Damanik, A., Ma, E., Wegman, D., 2011. Probing Lepton Flavor Triality with Higgs Boson Decay. *Phys. Rev. D* 83, 093012. doi:[10.1103/PhysRevD.83.093012](#), [arXiv:1103.0008](#).
- [32] Cepeda, M., et al., 2019. Report from Working Group 2: Higgs Physics at the HL-LHC and HE-LHC. CERN Yellow Rep. Monogr. 7, 221–584. doi:[10.23731/CYRM-2019-007.221](#), [arXiv:1902.00134](#).

- [33] Cheng, H., et al. (CEPC Physics Study Group), 2022. The Physics potential of the CEPC. Prepared for the US Snowmass Community Planning Exercise (Snowmass 2021), in: Snowmass 2021. [arXiv:2205.08553](#).
- [34] Christensen, N.D., de Aquino, P., Degrande, C., Duhr, C., Fuks, B., Herquet, M., Maltoni, F., Schumann, S., 2011. A Comprehensive approach to new physics simulations. *Eur. Phys. J. C* 71, 1541. doi:[10.1140/epjc/s10052-011-1541-5](#), [arXiv:0906.2474](#).
- [35] Crivellin, A., Ghezzi, M., Panizzi, L., Pruna, G.M., Signer, A., 2019. Low- and high-energy phenomenology of a doubly charged scalar. *Phys. Rev. D* 99, 035004. doi:[10.1103/PhysRevD.99.035004](#), [arXiv:1807.10224](#).
- [36] Dainese, A., Mangano, M., Meyer, A.B., Nisati, A., Salam, G., Vesterinen, M.A. (Eds.), 2019. Report on the Physics at the HL-LHC, and Perspectives for the HE-LHC. volume 7/2019 of *CERN Yellow Reports: Monographs*. CERN, Geneva, Switzerland. doi:[10.23731/CYRM-2019-007](#).
- [37] Das, D., Santamaria, A., 2016. Updated scalar sector constraints in the Higgs triplet model. *Phys. Rev. D* 94, 015015. doi:[10.1103/PhysRevD.94.015015](#), [arXiv:1604.08099](#).
- [38] Dawson, S., Valencia, G., 1995. Bounds on anomalous gauge boson couplings from partial Z widths at LEP. *Nucl. Phys. B* 439, 3–22. doi:[10.1016/0550-3213\(95\)00042-Q](#), [arXiv:hep-ph/9410364](#).
- [39] Dawson, S., et al., 2022. Report of the Topical Group on Higgs Physics for Snowmass 2021: The Case for Precision Higgs Physics, in: Snowmass 2021. [arXiv:2209.07510](#).
- [40] Dong, M., et al. (CEPC Study Group), 2018. CEPC Conceptual Design Report: Volume 2 - Physics & Detector [arXiv:1811.10545](#).
- [41] de Florian, D., et al. (LHC Higgs Cross Section Working Group), 2016. Handbook of LHC Higgs Cross Sections: 4. Deciphering the Nature of the Higgs Sector 2/2017. doi:[10.23731/CYRM-2017-002](#), [arXiv:1610.07922](#).
- [42] Fuks, B., Nemevšek, M., Ruiz, R., 2020. Doubly Charged Higgs Boson Production at Hadron Colliders. *Phys. Rev. D* 101, 075022. doi:[10.1103/PhysRevD.101.075022](#), [arXiv:1912.08975](#).
- [43] Gao, J. (CEPC Accelerator Study Group), 2022. Snowmass2021 White Paper AF3-CEPC [arXiv:2203.09451](#).
- [44] Gunion, J.F., Haber, H.E., Kane, G.L., Dawson, S., 2000. The Higgs Hunter’s Guide. volume 80.
- [45] Hahn, T., 2001. Generating Feynman diagrams and amplitudes with FeynArts 3. *Comput. Phys. Commun.* 140, 418–431. doi:[10.1016/S0010-4655\(01\)00290-9](#), [arXiv:hep-ph/0012260](#).

- [46] Hahn, T., Perez-Victoria, M., 1999. Automatized one loop calculations in four-dimensions and D-dimensions. *Comput. Phys. Commun.* 118, 153–165. doi:[10.1016/S0010-4655\(98\)00173-8](https://doi.org/10.1016/S0010-4655(98)00173-8), [arXiv:hep-ph/9807565](https://arxiv.org/abs/hep-ph/9807565).
- [47] Hamada, Y., Kitano, R., Matsudo, R., Takaura, H., Yoshida, M., 2022. μ TRISTAN. *PTEP* 2022, 053B02. doi:[10.1093/ptep/ptac059](https://doi.org/10.1093/ptep/ptac059), [arXiv:2201.06664](https://arxiv.org/abs/2201.06664).
- [48] He, X.G., Huang, Z.L., Li, M.W., Liu, C.W., 2024. The SM expected branching ratio for $h \rightarrow \gamma\gamma$ and an excess for $h \rightarrow Z\gamma$. *JHEP* 10, 135. doi:[10.1007/JHEP10\(2024\)135](https://doi.org/10.1007/JHEP10(2024)135), [arXiv:2402.08190](https://arxiv.org/abs/2402.08190).
- [49] He, X.G., Keum, Y.Y., Volkas, R.R., 2006. A(4) flavor symmetry breaking scheme for understanding quark and neutrino mixing angles. *JHEP* 04, 039. doi:[10.1088/1126-6708/2006/04/039](https://doi.org/10.1088/1126-6708/2006/04/039), [arXiv:hep-ph/0601001](https://arxiv.org/abs/hep-ph/0601001).
- [50] Holthausen, M., Lindner, M., Schmidt, M.A., 2013. Lepton flavor at the electroweak scale: A complete A_4 model. *Phys. Rev. D* 87, 033006. doi:[10.1103/PhysRevD.87.033006](https://doi.org/10.1103/PhysRevD.87.033006), [arXiv:1211.5143](https://arxiv.org/abs/1211.5143).
- [51] Hong, T.T., Le, V.K., Phuong, L.T.T., Hoi, N.C., Ngan, N.T.K., Nha, N.H.T., 2024. Decays of Standard Model–Like Higgs Boson $h \rightarrow \gamma\gamma, Z\gamma$ in a Minimal Left-Right Symmetric Model. *PTEP* 2024, 033B04. doi:[10.1093/ptep/ptae029](https://doi.org/10.1093/ptep/ptae029), [arXiv:2312.11045](https://arxiv.org/abs/2312.11045). [Erratum: *PTEP* 2024, 059201 (2024)].
- [52] Kannike, K., 2012. Vacuum Stability Conditions From Copositivity Criteria. *Eur. Phys. J. C* 72, 2093. doi:[10.1140/epjc/s10052-012-2093-z](https://doi.org/10.1140/epjc/s10052-012-2093-z), [arXiv:1205.3781](https://arxiv.org/abs/1205.3781).
- [53] Lavoura, L., 2003. General formulae for $f(1) \rightarrow f(2) \gamma$. *Eur. Phys. J. C* 29, 191–195. doi:[10.1140/epjc/s2003-01212-7](https://doi.org/10.1140/epjc/s2003-01212-7), [arXiv:hep-ph/0302221](https://arxiv.org/abs/hep-ph/0302221).
- [54] Li, T., Schmidt, M.A., 2019a. Sensitivity of future lepton colliders and low-energy experiments to charged lepton flavor violation from bileptons. *Phys. Rev. D* 100, 115007. doi:[10.1103/PhysRevD.100.115007](https://doi.org/10.1103/PhysRevD.100.115007), [arXiv:1907.06963](https://arxiv.org/abs/1907.06963).
- [55] Li, T., Schmidt, M.A., 2019b. Sensitivity of future lepton colliders to the search for charged lepton flavor violation. *Phys. Rev. D* 99, 055038. doi:[10.1103/PhysRevD.99.055038](https://doi.org/10.1103/PhysRevD.99.055038), [arXiv:1809.07924](https://arxiv.org/abs/1809.07924).
- [56] Lichtenstein, G., Schmidt, M.A., Valencia, G., Volkas, R.R., 2023. Complementarity of μ TRISTAN and Belle II in searches for charged-lepton flavour violation. *Phys. Lett. B* 845, 138144. doi:[10.1016/j.physletb.2023.138144](https://doi.org/10.1016/j.physletb.2023.138144), [arXiv:2307.11369](https://arxiv.org/abs/2307.11369).
- [57] de Melo, T.B., Queiroz, F.S., Villamizar, Y., 2019. Doubly Charged Scalar at the High-Luminosity and High-Energy LHC. *Int. J. Mod. Phys. A* 34, 1950157. doi:[10.1142/S0217751X19501574](https://doi.org/10.1142/S0217751X19501574), [arXiv:1909.07429](https://arxiv.org/abs/1909.07429).

- [58] Mertig, R., Bohm, M., Denner, A., 1991. FEYN CALC: Computer algebraic calculation of Feynman amplitudes. *Comput. Phys. Commun.* 64, 345–359. doi:[10.1016/0010-4655\(91\)90130-D](https://doi.org/10.1016/0010-4655(91)90130-D).
- [59] Mlynarikova, M. (ATLAS, CMS), 2023. Higgs Physics at HL-LHC, in: 30th International Workshop on Deep-Inelastic Scattering and Related Subjects. [arXiv:2307.07772](https://arxiv.org/abs/2307.07772).
- [60] Morel, L., Yao, Z., Cladé, P., Guellati-Khélifa, S., 2020. Determination of the fine-structure constant with an accuracy of 81 parts per trillion. *Nature* 588, 61–65. doi:[10.1038/s41586-020-2964-7](https://doi.org/10.1038/s41586-020-2964-7).
- [61] Muramatsu, Y., Nomura, T., Shimizu, Y., 2016. Mass limit for light flavon with residual Z_3 symmetry. *JHEP* 03, 192. doi:[10.1007/JHEP03\(2016\)192](https://doi.org/10.1007/JHEP03(2016)192), [arXiv:1601.04788](https://arxiv.org/abs/1601.04788).
- [62] Nowakowski, M., Paschos, E.A., Rodriguez, J.M., 2005. All electromagnetic form-factors. *Eur. J. Phys.* 26, 545–560. doi:[10.1088/0143-0807/26/4/001](https://doi.org/10.1088/0143-0807/26/4/001), [arXiv:physics/0402058](https://arxiv.org/abs/physics/0402058).
- [63] Parker, R.H., Yu, C., Zhong, W., Estey, B., Müller, H., 2018. Measurement of the fine-structure constant as a test of the Standard Model. *Science* 360, 191. doi:[10.1126/science.aap7706](https://doi.org/10.1126/science.aap7706), [arXiv:1812.04130](https://arxiv.org/abs/1812.04130).
- [64] Pascoli, S., Zhou, Y.L., 2016. Flavon-induced connections between lepton flavour mixing and charged lepton flavour violation processes. *JHEP* 10, 145. doi:[10.1007/JHEP10\(2016\)145](https://doi.org/10.1007/JHEP10(2016)145), [arXiv:1607.05599](https://arxiv.org/abs/1607.05599).
- [65] Patel, H.H., 2015. Package-X: A Mathematica package for the analytic calculation of one-loop integrals. *Comput. Phys. Commun.* 197, 276–290. doi:[10.1016/j.cpc.2015.08.017](https://doi.org/10.1016/j.cpc.2015.08.017), [arXiv:1503.01469](https://arxiv.org/abs/1503.01469).
- [66] Patel, H.H., 2017. Package-X 2.0: A Mathematica package for the analytic calculation of one-loop integrals. *Comput. Phys. Commun.* 218, 66–70. doi:[10.1016/j.cpc.2017.04.015](https://doi.org/10.1016/j.cpc.2017.04.015), [arXiv:1612.00009](https://arxiv.org/abs/1612.00009).
- [67] Ruiz, R., 2022. Doubly charged Higgs boson production at hadron colliders II: a Zee-Babu case study. *JHEP* 10, 200. doi:[10.1007/JHEP10\(2022\)200](https://doi.org/10.1007/JHEP10(2022)200), [arXiv:2206.14833](https://arxiv.org/abs/2206.14833).
- [68] Schael, S., et al. (ALEPH, DELPHI, L3, OPAL, SLD, LEP Electroweak Working Group, SLD Electroweak Group, SLD Heavy Flavour Group), 2006. Precision electroweak measurements on the Z resonance. *Phys. Rept.* 427, 257–454. doi:[10.1016/j.physrep.2005.12.006](https://doi.org/10.1016/j.physrep.2005.12.006), [arXiv:hep-ex/0509008](https://arxiv.org/abs/hep-ex/0509008).
- [69] Schwartz, M.D., 2014. *Quantum Field Theory and the Standard Model*. Cambridge University Press.
- [70] Shtabovenko, V., 2017. FeynHelpers: Connecting FeynCalc to FIRE and Package-X. *Comput. Phys. Commun.* 218, 48–65. doi:[10.1016/j.cpc.2017.04.014](https://doi.org/10.1016/j.cpc.2017.04.014), [arXiv:1611.06793](https://arxiv.org/abs/1611.06793).

- [71] Shtabovenko, V., Mertig, R., Orellana, F., 2016. New Developments in FeynCalc 9.0. *Comput. Phys. Commun.* 207, 432–444. doi:[10.1016/j.cpc.2016.06.008](https://doi.org/10.1016/j.cpc.2016.06.008), [arXiv:1601.01167](https://arxiv.org/abs/1601.01167).
- [72] Shtabovenko, V., Mertig, R., Orellana, F., 2020. FeynCalc 9.3: New features and improvements. *Comput. Phys. Commun.* 256, 107478. doi:[10.1016/j.cpc.2020.107478](https://doi.org/10.1016/j.cpc.2020.107478), [arXiv:2001.04407](https://arxiv.org/abs/2001.04407).
- [73] Shtabovenko, V., Mertig, R., Orellana, F., 2025. FeynCalc 10: Do multiloop integrals dream of computer codes? *Comput. Phys. Commun.* 306, 109357. doi:[10.1016/j.cpc.2024.109357](https://doi.org/10.1016/j.cpc.2024.109357), [arXiv:2312.14089](https://arxiv.org/abs/2312.14089).
- [74] Xu, F., 2023. Neutral and doubly charged scalars at future lepton colliders. *Phys. Rev. D* 108, 036002. doi:[10.1103/PhysRevD.108.036002](https://doi.org/10.1103/PhysRevD.108.036002), [arXiv:2302.08653](https://arxiv.org/abs/2302.08653).
- [75] Zee, A., 1986. Quantum Numbers of Majorana Neutrino Masses. *Nucl. Phys. B* 264, 99–110. doi:[10.1016/0550-3213\(86\)90475-X](https://doi.org/10.1016/0550-3213(86)90475-X).